Journal of Enzyme Inhibition and Medicinal Chemistry, 2010; 25(5): 615–621

informa
healthcare

ORIGINAL ARTICLE

Synthesis and biological activity of pyrazolo[3,4-*d*]thiazolo[3,2-*a*]pyrimidin-4-one derivatives: *in silico* approach

Chandrahas N. Khobragade[1], Ragini G. Bodade[1], Bhaskar S. Dawane[2], Shankaraiah G. Konda[2], and Namdev T. Khandare[2]

[1]*Biochemistry Research Laboratory, School of Life Sciences, Swami Ramanand Teerth Marathwada University, Nanded, India, and* [2]*Organic Chemistry Research Laboratory, Department of Chemistry, Yeshwant Mahavidyalaya, Nanded, India*

Abstract

Xanthine oxidase (XO) is responsible for the pathological condition called gout. Inhibition of XO activity by various pyrazolo[3,4-*d*]thiazolo[3,2-*a*]pyrimidine-4-one derivatives was assessed and compared with the standard inhibitor allopurinol. Out of 10 synthesized compounds, two compounds, viz. 3-amino-6-(2-hydroxyphenyl)-1*H*-pyrazolo[3,4-*d*]thiazolo[3,2-*a*]pyrimidin-4-one (**3b**) and 3-amino-6-(4-chloro-2-hydroxy-5-methylphenyl)-1*H*-pyrazolo[3,4-*d*]thiazolo[3,2-*a*]pyrimidin-4-one (**3g**) were found to have promising XO inhibitory activity of the same order as allopurinol. Both compounds and allopurinol inhibited competitively with comparable K*i* (**3b**: 3.56 µg, **3g**: 2.337 µg, allopurinol: 1.816 µg) and IC_{50} (**3b**: 4.228 µg, **3g**: 3.1 µg, allopurinol: 2.9 µg) values. The enzyme–ligand interaction was studied by molecular docking using Autodock in BioMed Cache V. 6.1 software. The results revealed a significant dock score for **3b** (−84.976 kcal/mol) and **3g** (−90.921 kcal/mol) compared with allopurinol (−55.01 kcal/mol). The physiochemical properties and toxicity of the compounds were determined *in silico* using online computational tools. Overall, *in vitro* and *in silico* study revealed 3-amino-6-(4-chloro-2-hydroxy-5-methylphenyl)-1*H*-pyrazolo[3,4-*d*]thiazolo[3,2–*a*]pyrimidin-4-one **(3g)** as a potential lead compound for the design and development of XO inhibitors.

Keywords: *Pyrazolo[3,4-d]thiazolo[3,2-a]pyrimidine-4-one; inhibitory activity; xanthine oxidase (XO); molecular modeling*

Introduction

Xanthine oxidase (XO, E.C. 1.1.3.22) is a key enzyme in the purine scavenging pathway and catalyzes the conversion of hypoxanthine to xanthine and xanthine to uric acid[1]. The enzyme is distributed widely in bacteria, higher plants, invertebrates, and vertebrates. In mammals the enzyme is present in the kidney, lungs, myocardium, brain, plasma, and erythrocytes; however, higher activity is found in the liver and intestine[2]. An increased level of xanthine oxidase (XO) is implicated in ischemic-reperfusion injury, renal stone formation, and reactive oxygen species (ROS) induced pathological states such as hepatitis, inflammation, aging, and carcinogenesis[3,4]. In addition to this, the overproduction of uric acid leads to hyperuricemia (>7 mg/dL) and gout[5]. Gout, a common rheumatic disease, is caused by the deposition of monosodium urate crystals (MSU) in synovial joints, with painful inflammation[6]. Moreover, gout is also associated with hypertension, hyperlipidation, diabetes mellitus, obesity, and cardiovascular diseases[7]. The prevalence of gout has been increasing worldwide during the past four decades, and affects nearly 1% of the population in Western countries[8–10]. The disease is found commonly in the UK, Japan, the Philippines, and Taiwan, and in Samoans, the Maori people of New Zealand, and Australian aborigines, with higher morbidity and mortality rates[11,12]. Treatment of gout involves the use of xanthine oxidoreductase (XOR) inhibitors and uricosuric agents[13,14]. Allopurinol, a potent suicide inhibitor, coordinates irreversibly with the reduced form of XO and blocks the terminal step in uric acid biosynthesis and lowers the plasma uric acid concentration. It is the only clinically

Address for Correspondence: Chandrahas N. Khobragade, Biochemistry Research Laboratory, School of Life Sciences, Swami Ramanand Teerth Marathwada University, Nanded-431606, India. Tel: 91(2462)229242. Fax: 91(2462)229245. E-mail: cnkhobragade@rediffmail.com

(Received 22 May 2009; revised 30 September 2009; accepted 06 October 2009)

ISSN 1475-6366 print/ISSN 1475-6374 online © 2010 Informa UK, Ltd.
DOI: 10.3109/14756360903389849

available XO inhibitor that has been widely used, because of its tolerance in patients[15,16]. However, allopurinol treatment produces several life-threatening hypersensitivity reactions such as Stevens–Johnson syndrome or toxic epidermal necrosis, and a variety of drug interactions[17,18]. Apart from allopurinol, several pteridines, thiazoles, phenyl pyrazoles, aryl triazoles, and flavonoids are reported to be inhibitors of XOR[19]. Therefore, the management of gout involves not only treating acute arthritic inflammation and urolithiasis but also lowering the urate levels, with the goal of preventing a recurrent disease state and its progression[20].

Pyrazolopyrimidines are well known for their pharmacological activities including antitumor, antipyretic, anticancer, antimicrobial, antiviral, anti-inflammatory, analgesic, antileishmanial, and antihistaminic activities[21,22]. They also exhibit central nervous system (CNS) depressant, neuroleptic, and anti-tuberculostatic activities[23]. Pyrazoles and other heterocyclic compounds also possess inhibitory activities against XO, cyclooxygenase (COX), and alkaline phosphatases[24–26].

Prompted by the diverse pharmacological activities of pyrazolopyrimidines and continuation of our search for more potent xanthine oxidase inhibitors, we report here the synthesis of pyrazolo[3,4-*d*]thiazolo[3,2-*a*]pyrimidin-4-one derivatives, bearing different functional moieties, and a study of their XO inhibitory activities. An attempt has been made to insert the thiazolo moiety in pyrazolopyrimidine derivatives for activity reinforcement.

Materials and methods

Materials

Xanthine, uric acid, nicotinamide adenine dinucleotide (NAD^+), nystatin, and tetracycline were purchased from HiMedia Laboratories Ltd., Mumbai, India. All chemicals were of AR grade and used without further purification unless stated otherwise. Bovine milk xanthine oxidase was purchased from Sigma Chemical Co. (St. Louis, MO).

Methods

Melting points of the synthesized compounds were obtained on a Kofler micro-melting point apparatus and were uncorrected. Thin layer chromatography (TLC) of all the derivatives was monitored on silica gel-G coated glass plates, and products were visualized by iodine vapor to check the purity. Infrared (IR) spectra were recorded on a Thermo Nicolet Nexus 670 spectrometer using KBr pellets. ^{1}H nuclear magnetic resonance (NMR) spectra were obtained using an Avance 300 MHz spectrophotometer in dimethylsulfoxide (DMSO)-d_6 with tetramethylsilane (TMS) as an internal standard (Table 1). In all cases chemical shifts are in ppm downfield to TMS.

Synthesis of 3-cyano-2–methylthio-4-oxo-4H–6-(substituted-phenyl)thiazolo[3,2-a]pyrimidine (2a–j)

Synthesis of the target molecule was carried out according to the reported procedure[27,28]. Equimolar quantities of 2-amino-4-(substituted phenyl)thiazoles (**1a–j**) (1 mM) and cyanoketene dithioacetal (1 mM) were refluxed in dry dimethyl formamide (DMF) in the presence of trimethylamine (TEA), which afforded the 3-cyano-2-methylthio-4-oxo-4*H*-substituted thiazolo[1,2-*a*]pyrimidines (**2a–j**). All the compounds were characterized by IR and ^{1}H NMR as follows.

Table 1. Structure of pyrazolopyrimidine derivatives.

	Substitutent					
Entry	R_1	R_2	R_3	R_4	Yield (%)	M.P. (°C)
3a	H	H	Cl	H	65	204
3b	OH	H	H	H	66	215
3c	OH	H	H	Cl	64	220
3d	OH	Br	H	Cl	65	195
3e	H	H	NO_2	H	66	202
3f	H	H	Br	H	66	202
3g	OH	H	Cl	CH_3	68	220
3h	OH	H	Cl	Cl	68	192
3i	H	H	OH	H	67	241
3j	OH	I	H	Cl	68	210

*3-Cyano-2-methylthio-4-oxo-4H-5-(4-chlorophenyl) thiazolo[1,2-a]pyrimidine (**2a**)* IR (KBr ν max): 2210 (C≡N), 1640 (C=O), 1598 (C=N) cm^{-1}; ^{1}H NMR (DMSO-d_6): δ 2.58 (s, 3H, SCH_3), δ 7.16 (s, 1H, 5H-thiazole), δ 7.31–7.67 (m, 4 H, Ar-H) ppm; Anal. Calculated: C, 50.37; H, 2.39; N, 12.50%. Found: C, 50.34; H, 2.43; N, 12.46%.

*3-Cyano-2-methylthio-4-oxo-4H-5-(2-hydroxyphenyl) thiazolo[1,2-a]pyrimidine (**2b**)* IR (KBr ν max): 3310 (OH), 2220 (C≡N), 1685 (C=O), 1602(C=N) cm^{-1}; ^{1}H NMR (DMSO-d_6): δ 11.08 (S, 1 H, OH), 2.61 (s, 3H, SCH_3), δ 7.15 (s, 1H, 5H-thiazole), δ 7.2–7.38 (m, 4H, Ar-H) ppm; Anal. Calculated: C, 53.33; H, 2.85; N, 13.33%. Found: C, 53.38; H, 2.81; N, 13.38%.

*3-Cyano-2-methylthio-4-oxo-4H-5-(5-chloro-2-hydroxyphenyl)thiazolo[1,2-a]pyrimidine (**2c**)* IR (KBr ν max): 3325 (OH), 2215 (C≡N), 1685 (C=O), 1605 (C=N) cm^{-1}; ^{1} H NMR (DMSO-d_6): δ 11.25 (s, 1 H, OH), 2.50 (s, 3H, SCH_3); δ 7.18 (s, 1H, 5H-thiazole), δ 7.28–7.5 (m, 3H, Ar-H) ppm; Anal. Calculated: C, 48.06; H, 2.28; N, 12.01%. Found: C, 48.02; H, 2.30; N, 12.05%.

Synthesis of 3-amino-6-(substituted-phenyl)-1H-pyrazolo[3,4-d]thiazolo[3,2-a]pyrimidin-4-one (3a–j)

Reaction of 3-cyano-2-methylthio-4-oxo-4*H*-substituted-thiazolo[1,2-*a*]pyrimidine (**2a–j**) with hydrazine hydrate in ethanolic solution was refluxed for 3 h. It afforded the pyrazolo[3,4-*d*]thiazolo[3,2-*a*]pyrimidin-4-one derivatives (Scheme 1). The solvent was removed and the residue was treated with chloroform and extracted with water. The chloroform layer was separated and concentrated. After complete evaporation of chloroform, compounds **3a–j** were obtained as colorless crystalline solids.

*3-Amino-6-(4-chlorophenyl)-1H-pyrazolo[3,4-d] thiazolo[3,2-a]pyrimidin-4-one (**3a**)* IR (KBr ν max): 3455 (NH), 3340 (NH_2), 3320 (-NH), 1660 (C=O), 1605 (C=N) cm^{-1} ^{1}H NMR (DMSO-d_6): δ 4.60 (bs, 2H, NH_2), δ 7.1 (s, 1H, 5H- thiazole), δ 7.31–7.64 (m 4H, Ar-H), δ 8.6 (s, 1H, NH) ppm; Anal. Calculated: C, 49.13; H, 2.51; N, 22.04%. Found: C, 49.16; H, 2.52; N, 22.08%.

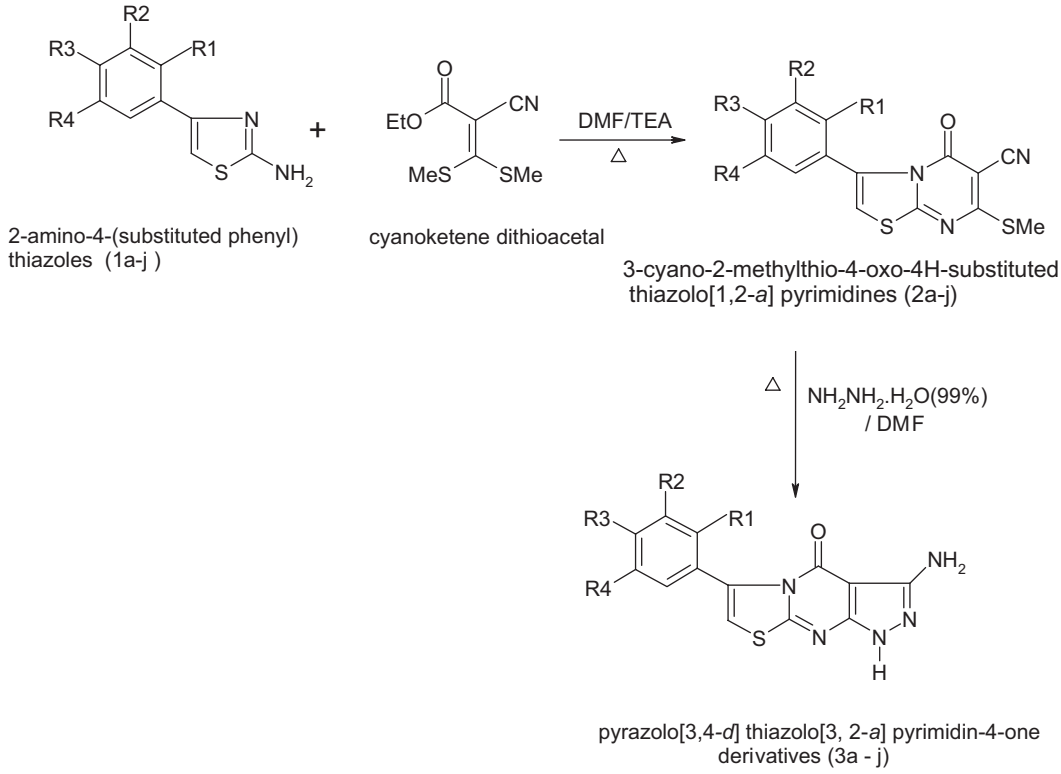

Scheme 1. Synthesis of pyrazolopyrimidine derivatives.

*3-Amino-6-(2-hydroxyphenyl)-1H-pyrazolo[3,4-d] thiazolo[3,2-a]pyrimidin-4-one (**3b**)* IR (KBr ν max): 3460 (NH), 3330 (NH_2), 3316 (-NH), 3210 (-OH), 1648 (C=O), 1608 (C=N) cm^{-1}. ^1H NMR (DMSO-d_6): δ 4.85 (bs, 2H, NH_2), δ 7.08 (s, 1H, 5H-thiazole), δ 7.36–7.72 (m, 4H, Ar-H), δ 8.4 (s, 1 H, NH), δ 11.56 (s, 1H, OH) ppm; Anal. Calculated: C, 52.17; H, 3.01; N, 23.41%. Found: C, 52.21; H, 3.04; N, 23.38%.

*3-Amino-6-(5-chloro-2-hydroxyphenyl)-1H-pyrazolo[3,4-d]thiazolo[3,2-a]pyrimidin-4-one (**3c**)* IR (KBr ν max): 3460 (NH), 3455 (NH_2), 3283 (-NH), 3192 (-OH), 1649 (C=O), 1613 (C=N) cm^{-1}. ^1H NMR (DMSO-d_6): δ 4.91 (bs, 2H, NH_2), δ 7.15 (s, 1H, 5H-thiazole), δ 7.31 (s, 1H, Ar-H), δ 7.54 (s, 1H, Ar-H), δ 7.82 (s, 1H, Ar-H), δ 8.36(s, 1H, NH), δ 11.46 (s, 1H, OH) ppm; Anal. Calculated: C, 46.77; H, 2.39; N, 20.98%. Found: C, 46.81; H, 2.32; N, 20.93%.

*3-Amino-6-(3-bromo-5-chloro-2-hydroxyphenyl)-1H-pyrazolo[3,4-d]thiazolo[3,2-a]pyrimidin-4-one (**3d**)* IR (KBr ν max): 3425 (NH), 3294 (NH_2), 3327.03 (-NH), 3185 (-OH), 1655 (C=O), 1608 (C=N) cm^{-1}. ^1H NMR (DMSO-d_6): δ 4.83 (bs, 2H, NH_2), δ 7.06 (s, 1H, 5H-thiazole), δ 7.50 (s, 1H, Ar-H), δ 7.81 (s, 1H, Ar-H), δ 8.51 (s, 1H, NH), δ 11.54 (s, 1H, OH) ppm; Anal. Calculated: C, 37.81; H, 1.69; N, 16.90%. Found: C, 37.84; H, 1.65; N, 16.846%.

*3–Amino-6-(4-nitrophenyl)-1H-pyrazolo[3,4-d] thiazolo[3,2-a]pyrimidin-4-one (**3e**)* IR (KBr ν max): 3387 (NH), 3256 (NH), 3256 (-NH), 2098 (N=O), 1658 (C=O), 1610 (C=N) cm^{-1}. ^1H NMR (DMSO-d_6): δ 4.85 (bs, 2H, NH_2), δ 7.12 (s, 1H, 5H-thiazole), δ 7.38–7.86 (m, 4H, Ar-H), δ 8.36 (s, 1H, NH) ppm; Anal. Calculated: C, 52.70; H, 2.70; N, 28.37%. Found: C, 52.74; H, 2.68; N, 28.35%.

*3-Amino-6-(4-bromophenyl)-1H-pyrazolo[3,4-d] thiazolo[3,2-a]pyrimidin-4-one (**3f**)* IR (KBr ν max): 3432 (NH), 3340.15 (-NH_2), 3340.15 (-NH), 3210 (OH), 1660 (C=O), 1609 (C=N) cm^{-1}. ^1H NMR (DMSO-d_6): δ 5.10 (bs, 2H, NH_2), δ 7.16 (s, 1H, 5H-thiazole), δ 7.35–7.82 (m, 4H, Ar-H), δ 8.31 (s, 1H, NH) ppm; Anal. Calculated: C, 43.09; H, 2.20; N, 19.33%. Found: C, 43.05; H, 2.16; N, 19.30%.

*3-Amino-6-(4-chloro-2-hydroxy-5-methylphenyl)-1H-pyrazolo[3,4-d]thiazolo[3,2-a]pyrimidin-4-one (**3g**)* IR (KBr ν max): 3334 (NH), 3300 (NH_2), 3385 (-NH), 3186 (-OH), 1665 (C=O), 1607.51 (C=N) cm^{-1}. ^1H NMR (DMSO-d_6): δ 2.15 (s, 3H, CH_3), δ 4.86 (bs, 2H, NH_2), δ 7.05 (s, 1H, 5H-thiazole), δ 7.81 (s, 1H, Ar-H), δ 7.42 (s, 1H, Ar-H), δ 8.51 (s, 1H, NH), δ 11.54 (s, 1H, OH) ppm; Anal. Calculated: C, 48.34; H, 2.87; N, 20.14%. Found: C, 48.35; H, 2.84; N, 20.16%.

*3-Amino-6-(4,5-dichloro-2-hydroxyphenyl)-1H-pyrazolo[3,4-d]thiazolo[3,2-a]pyrimidin-4-one (**3h**)* IR (KBr ν max): 3410 (-NH), 3376 (-NH_2), 3195 (-OH), 1655 (C=O), 1604.51 (C=N) cm^{-1}. ^1H NMR (DMSO-d_6): δ 4.91 (bs, 2H, NH_2), δ 7.16 (s, 1H, 5H-thiazole), δ 7.43 (s, 1H, Ar-H), δ 7.82 (s, 1H, Ar-H), δ 8.32 (s, 1H, NH), δ 11.82 (s, 1H, OH) ppm; Anal. Calculated: C, 42.50; H, 1.90; N, 19.07%. Found: C, 42.54; H, 1.93; N, 19.02%.

*3-Amino-6-(4-hydroxyphenyl)-1H-pyrazolo[3,4-d] thiazolo[3,2-a]pyrimidin-4-one (**3i**)* IR (KBr ν max): 3402 (-NH), 3360 (-NH_2), 3243 (OH), 1642 (C=O), 1660 (C=N) cm^{-1}. ^1H NMR (DMSO-d_6): δ 5.05 (bs, 2H, NH_2), δ 6.22 (s. 1H, OH), δ 7.05 (s, 1H, 5H-thiazole), δ 7.41–7.86 (m, 4H, Ar-H), δ 8.41 (s, 1H, NH) ppm; Anal. Calculated: C, 52.17; H, 3.01; N, 23.41%. Found: C, 52.14; H, 3.05; N, 23.46%.

*3-Amino-6-(5-chloro-2-hydroxy-3-iodophenyl)-1H-pyrazolo[3,4-d]thiazolo[3,2-a]pyrimidin-4-one (**3j**)* IR (KBr ν max): 3385(-NH), 3286 (-NH_2), 3192 (-OH), 1665 (C=O), 1606.51 (C=N) cm^{-1}. ^1H NMR (DMSO-d_6): δ 4.87 (bs, 2H, NH_2), δ 7.12 (s, 1H, 5H-thiazole), δ 7.85 (s, 1H, Ar-H), δ 7.51 (s, 1H, Ar-H), δ 8.52 (s, 1H, NH), δ 11.64 (s, 1H, OH) ppm; Anal. Calculated: C, 33.94; H, 1.52; N, 15.23%. Found: C, 33.91; H, 1.56; N, 15.20%.

Xanthine oxidase inhibitory activity

A series of 10 pyrazolopyrimidine derivatives synthesized in this study were tested as inhibitors. The reaction mixture containing 1 mL xanthine (0.15 mM), 2.5 mL potassium phosphate buffer (50 mM, pH 7.4), and 0.5 mL of XO solution (0.405 U/mL) was incubated for 5 min at room temperature. Uric acid formation was recorded at 293 nm using a spectrophotometer (UV-Vis Shimadzu 1601). The inhibitory effect of all the derivatives was determined by quantifying the amount of uric acid (UA) produced from xanthine. A decrease in UA formation at 293 nm by a derivative in a reaction mixture confirmed XO inhibition. The concentration of UA was estimated by standard uric acid curve. The blank was prepared without enzyme solution. One unit of XO is defined as the amount of enzyme that produces 1 µmol of uric acid per minute at room temperature using 0.1 µM xanthine as substrate[29,30]. Kinetics study was carried out in the absence and presence of the derivatives with varying concentration of xanthine as substrate, i.e. 1–5 µg/mL (Table 2). The results were compared with standard inhibitor allopurinol. XO activity was expressed as percentage inhibition of XO, as:

$$\text{Inhibition rate I}(\%) = (C - S/C) \times 100$$

where S and C represent the absorbances of test compound and blank, respectively.

The IC_{50} values, i.e. the µg concentration of inhibitor necessary for 50% inhibition, were determined by reported procedure[31].

Molecular modeling

The three-dimenaional (3D) structure of milk XO complexed with febuxostat (Protein Data Bank (PDB) code: 1n5x) was selected from the National Center for Biotechnology Information (NCBI) database and the target site was identified for docking. The structure was refined using MM3 in the BioMed Cache (V. 6.1) software package[32]. All the calculations were performed on a Pentium III workstation. The inhibitor-binding region was defined by selecting a subset of residues within 5 Å of the location of the ligand (febuxostat TEI-6720) in the crystal structure. The structures of all the synthesized compounds, allopurinol, and febuxostat (TEI-6720) were refined at the lowest energy conformation. Compounds were then docked using rigid body docking to search for favorable binding alterations based on the interaction force field scoring that includes van der Waals and electrostatic interactions. The highest scoring orientation (dock score) for each ligand proposed a feasible binding mode of the inhibitor in the active site of XO (Table 3).

In silico drug-relevant properties and toxicities of all the compounds were also studied using open-source computational software (OSIRIS, PASS).

Results

The synthesis of 10 pyrazolo[3,4-*d*]thiazolo[3,2-*a*]-pyrimidin-4-one derivatives was carried out by replacing 1*H* of the pyrimidine moieties (Table 1). The yields for these reactions are from fair to good (60–70%).

In vitro xanthine oxidase inhibitory activity of all the derivatives was determined. The enzyme inhibition kinetics were analyzed by Lineweaver–Burk double reciprocal plots for the synthesized derivatives, and are depicted in Figures 1–3. The kinetics study revealed that both derivatives **3g** and **3b** inhibited XO activity competitively, with K*i* values 2.337 µg and 3.56 µg, respectively. Overall, the derivative **3g** was found to be a more effective inhibitor than **3b**, and similar to the standard allopurinol (K*i* value 1.816 µg). The percentage inhibition and IC_{50} were calculated for each test compound.

Both compounds inhibited the enzyme in the range of 50–60% at 3 µg/mL, as compared to allopurinol (66%) (Table 2). Hence, the substitution of groups such as halo, methyl, and hydroxyl is confirmed to confer inhibitory activity.

Molecular modeling represents a powerful way to design new candidate drugs by comparing the interactions of ligand molecules and proteins with those of active compounds. The compounds that were most likely to have high binding affinities were represented by dock scores. The compounds under study were also checked for their *in silico* enzyme inhibitory activity by docking on XO. The docking is in the active site at the molybdopterin domain of the enzyme. The derivatives were superimposed with the standard inhibitor febuxostat (TEI-6720) and the electron binding energy (dock score) was calculated, as depicted in Table 3.

Table 2. K*i* and IC_{50} values of the inhibitors.

Sr. no.	Inhibitor	Type of inhibition	K*i* value (µg/mL)	IC_{50} value (µg)	% Inhibition
1	3-Amino-6-(2-hydroxy phenyl)-1*H*-pyrazolo[3,4-*d*] thiazolo[3,2-*a*]pyrimidin-4-one **(3b)**	Competitive	3.56	4.228	59
2	3-Amino-6-(2-hydroxy-4-chloro-5-methylphenyl)-1*H*-pyrazolo[3,4-*d*]thiazolo[3,2-*a*]pyrimidin-4-one (**3g**)	Competitive	2.337	3.1	58
3	Allopurinol	Competitive	1.816	2.9	66

Table 3. Physicochemical properties and docking values of pyrazolo[3,4-*d*]thiazolo[3,2-*a*]pyrimidin-4-one derivatives.

Compound	Functional groups	Molecular formula	Molecular weight	Log P	Solubility	Mutagenicity	HBD	HBA	Pa	Dock score	Drug score
3a	Cl	$C_{13}H_{10}ClN_5OS$	319	0.75	−3.86	Non-mutagenic	3	4	0.404	−83.2	0.83
3b	OH,	$C_{13}H_{11}N_5O_2S$	301.06	−0.16	−2.82	Non-mutagenic	4	5	0.329	−85	0.9
3c	OH, Cl	$C_{13}H_{10}ClN_5O_2S$	335.02	0.45	−3.56	Non-mutagenic	4	5	0.358	−80.4	0.84
3d	Br,OH, Cl	$C_{13}H_9BrClN_5O_2S$	413	1.15	−4.39	Non-mutagenic	4	5	0.356	−80	0.68
3e	NO_2	$C_{13}H_{12}N_6O_3S$	332.07	−0.43	−3.46	Slightly mutagenic	5	6	0.346	−85.4	0.83
3f	Br	$C_{13}H_{10}BrN_5OS$	362.98	0.54	−3.66	Non-mutagenic	3	4	0.316	−78.3	0.78
3g	OH,Cl, CH_3	$C_{14}H_{12}ClN_5O_2S$	349	0.77	−3.9	Non-mutagenic	4	5	0.356	−90.9	0.79
3h	OH,Cl, Cl	$C_{13}H_9Cl_2N_5O_2S$	369	1.06	−4.3	Non-mutagenic	4	5	0.359	−85.6	0.74
3i	OH	$C_{13}H_{11}N_5O_2S$	301.06	−0.16	−2.82	Non-mutagenic	4	5	0.329	−87.3	0.54
3j	OH, I, Cl	$C_{13}H_9ClIN_5O_2S$	461	1.38	−4.58	Non-mutagenic	4	5	0.321	−86.4	0.64
Allopurinol	—	$C_5H_4N_4O$	136.04	−2.78	−1.54	Non-mutagenic	2	3	0.8	−55	0.95
Febuxostat	—	$C_{16}H_{16}N_2O_3S$	316.09	2.96	−2.63	Non-mutagenic	1	6	0.782	−96	0.67

In drug design, the compounds under study are usually screened to qualify a drug candidate depending upon their physiochemical properties set by the Lipinski "rule of five." In the present work, the physiochemical properties, viz. molecular weight, Log P values, solubility, mutagenicity, Pa (possibility of activity), hydrogen bond acceptors (HBA), hydrogen bond donors (HBD), and drug scores were calculated using online drug-relevant prediction property software (PASS, OSIRIS)[33,34].

Compounds **3b** and **3g** revealed good dock scores (−84.976 kcal/mol, −90.921 kcal/mol) and drug scores (0.9, 0.79), and therefore are considered to be better inhibitors of XO.

Discussion

Enzyme activity of the compounds **3b** and **3g** was calculated in terms of K*i* and IC_{50} values. Both compounds showed a competitive type of inhibition by binding with the free enzyme. Furthermore, an increase in substrate concentration caused a reversible enzyme inhibition. The parameter K*i* denotes the affinity of an enzyme towards an inhibitor; the greater the value of K*i*, the less is the binding affinity. The value depends on the substituted groups on the pyrazole ring. The IC_{50} value denotes the concentration of drug required to inhibit the enzyme activity by 50%. The results revealed that compound **3g** possesses a promising inhibitory activity in the same order as that of allopurinol.

To gain further insight into how the inhibitor interacts with the XO, molecular docking on XO (PDB: 1n5x) was performed using Autodock in BioMed Cache V. 6.1 software. The 3D structure of bovine XO complexed with febuxostat (TEI-6720) was selected, and the target site was identified for docking. The inhibitor-binding region was defined by selecting a subset of residues within 5 Å of the location of the ligand in the crystal structure. All the compounds were then docked using rigid body docking alterations based on the interaction force field scoring that includes van der Waals and electrostatic interactions. The highest scoring orientation for each ligand proposed a feasible binding mode of the inhibitor in the active site

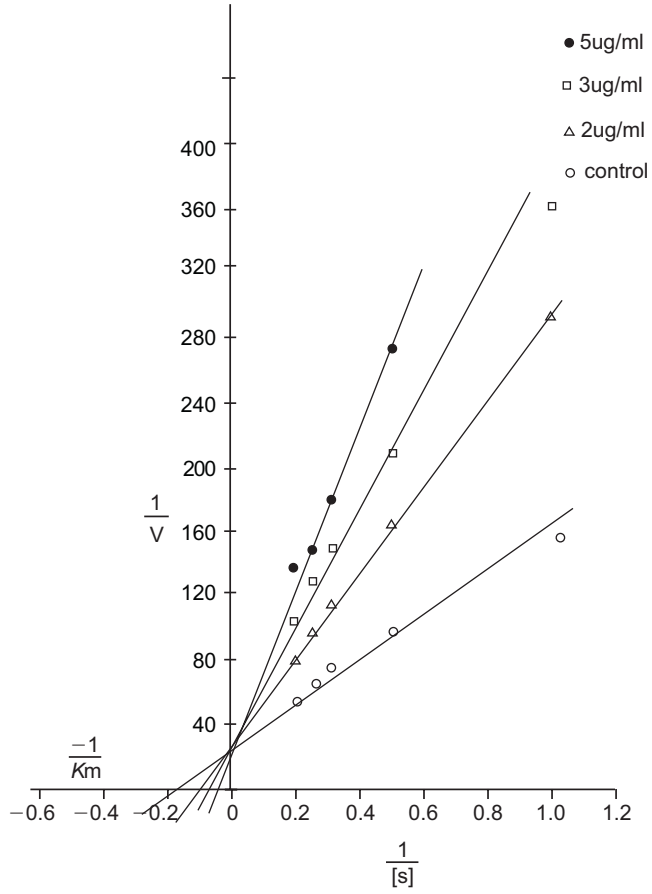

Figure 1. Lineweaver–Burk plot showing competitive inhibition of XO by derivative **3b** with varying concentration of xanthine (1–5 µg/mL) and fixed concentration of enzyme (0.0405 U/mL) in potassium phosphate buffer (50 mM, pH 7.4) to a total reaction volume of 3.5 mL.

of XO (Table 3). A significant dock score for **3b** (−84.976) and **3g** (−90.921) compared with allopurinol (−55.01) was observed. The observed result coincides with the above-reported *in vitro* enzyme inhibitory activity of **3b** and **3g**. In the enzyme–ligand interactions, amino acids of the active site Leu 648, Phe 649, Asn 768, Lys 771, Glu 802, Thr 803, Leu 873, Ser 876, Arg 880, Phe 914, Ser 1008, Phe 1009, Thr 1010, Val 1011, Phe 1013, Leu 1014, Pro 1076,

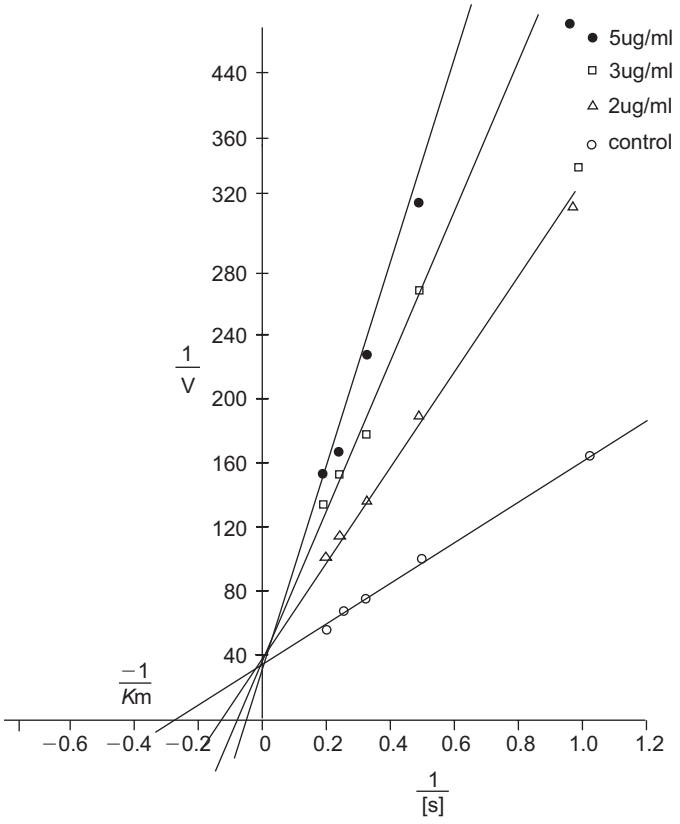

Figure 2. Lineweaver–Burk plot showing competitive inhibition of XO by derivative **3g** with varying concentration of xanthine (1–5 µg/mL) and fixed concentration of enzyme (0.0405 U/mL) in potassium phosphate buffer (50 mM, pH 7.4) to a total reaction volume of 3.5 mL.

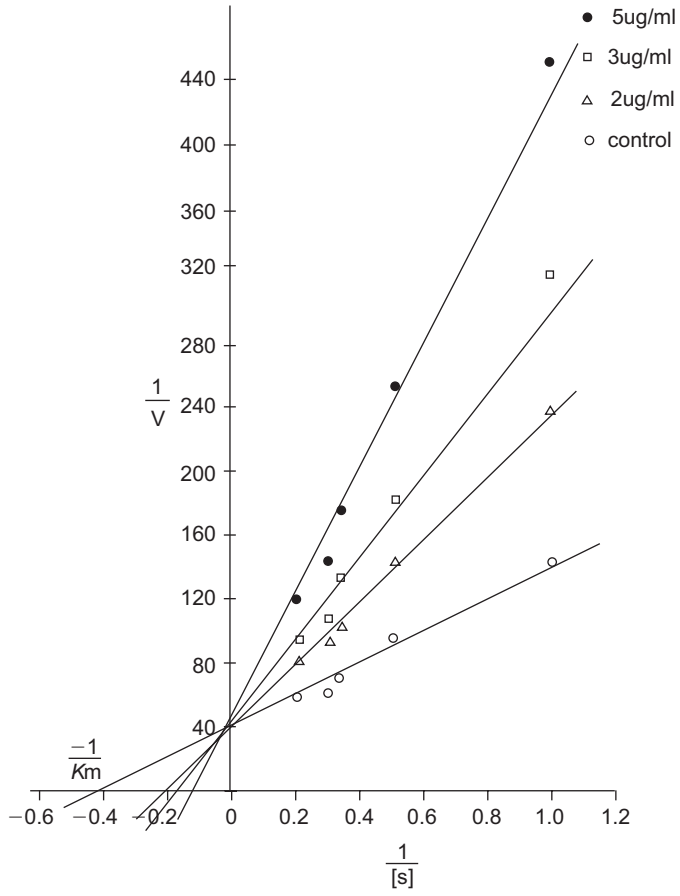

Figure 3. Lineweaver–Burk plot showing competitive inhibition of XO by allopurinol with varying concentration of xanthine (1–5 µg/mL) and fixed concentration of enzyme (0.0405 U/mL) in potassium phosphate buffer (50 mM, pH 7.4) to a total reaction volume of 3.5 mL.

Ala 1078, Ala 1079, and Glu 1261 were found to stack on the majority of compounds. Replacement of the hydrogen acceptor groups by hydrogen donors may increase the binding of the active site. This study permits the screening of molecules for future investigation.

Prediction of toxicity, drug likeness, and drug score by the computer program OSIRIS provides the basis for avoiding the experimental study of potentially harmful substances. In OSIRIS, toxicity risk assessment predicts mutagenicity, tumorigenicity, and irritant and reproductive effects. Prediction of biological activity spectra for the synthesized compounds was performed by PASS. This covers 1482 kinds of biological activities including basic pharmacological effects, action mechanisms, and specific toxicities. The result of prediction is presented as a list of activities with appropriate Pa and Pi values. Pa and Pi are estimates of probabilities for the compound to be active and inactive, respectively, for each type of activity from the biological activity spectrum.

Lipophilicity was also determined *in silico* using OSIRIS. The lipophilicity of a compound (Log P) is associated with its transport across the various bio-membranes. All the compounds were found to be within the range of lipophilicity (>5) as compared to the standard. According to the Lipinski "rule of five," solubility and molecular weight of a compound are related to its excretion and *in vivo* administration. Acceptable solubility (>5) and molecular weight (>500) were observed for all the compounds. Toxicity of a compound is determined in the form of mutagenicity, tumorigenicity, and irritant and reproductive effects. The results summarized in Table 2 revealed all compounds to be non-mutagenic, and therefore biologically safe for administration. It is reported that some nitro compounds may possess carcinogenicity and mutagenicity[35]. This might be the reason that compound **3e** was revealed to be slightly mutagenic and tumorigenic. Compounds **3a–j** showed an HBA level below 10 and HBD below 5, which are also within the limits set by the Lipinski rule. Overall, the compounds possessed a good drug score as compared to the standard inhibitor allopurinol. The drug novelty of the compounds was determined by their Pa values. Even though all the compounds under study showed a structure–activity relationship with the compound allopurinol, they showed novelty (>0.5), compared with allopurinol (0.800).

In summary, we have described the synthesis and XO inhibitory activity of pyrazolothiazolopyrimidine based inhibitors. Molecular docking and drug likeness of the compounds confirmed 3-amino-6-(4-chloro-2-hydroxy-5-methylphenyl)-1*H*-pyrazolo[3,4-*d*]thiazolo[3,2-*a*]-pyrimidin-4-one as a future lead compound for the design

and development of XOR inhibitors in the treatment of hyperuricemia and gout.

Acknowledgements

The authors are thankful to the Director and Head, School of Life Sciences, SRTM University, Nanded for providing necessary facilities.

Declaration of interest

One of the author Ms. Ragini G. Bodade gratefully acknowledge the University Grants Commission (UGC) New Delhi, India for financial assistance in the form of Rajiv Gandhi National Fellowship.

References

1. Ling L. Xanthine oxidase. Free Radic Biol Med 2001;77(222):1–10.
2. Khobragade CN, Bodade RG, Shinde MS, Jaju DR, Bhosle RB, Dawane BS. Microbial and xanthine dehydrogenase inhibitory activity of some flavones. J Enzyme Inhib Med Chem 2008;23:341–6.
3. Rundles RW, Wyngaarden JB, Hitchings GH, Elion GB. Drugs and uric acid. Annu Rev Pharmacol 1969;9:345–62.
4. Tamta H, Kalra S, Mukhopadhyay AK. Biochemical characterization of some pyrazolpyrimidine-based inhibitors of xanthine oxidase. Biochem 2006;71:S49–54.
5. Choil HK, Mount DB, Reginato AM. Pathogenesis of gout. Ann Intern Med 2005;143:499–516.
6. Choi HK, Curhan G. Gout: epidemiology and lifestyle choices. Curr Opin Rheumatol 2005;17:341–5.
7. Wortmann RL. Gout and hyperuricemia. Curr Opin Rheumatol 2002;14:281–6.
8. Terkeltaub RA. Gout in 2006. Bull NYU Hosp Jt Dis 2006;64:82–6.
9. Saag KG, Mikuls TR. Recent advances in the epidemiology of gout. Curr Rheumatol Rep 2005;7:235–41.
10. Lawrence RC, Helmick CG, Arnett FC. Estimation of the prevalence of arthritis and selected musculoskeletal disorders in the US. Arth Rheumtol 1998;41:778–99.
11. Mikuls TR, Farrar JT, Bilker WB, et.al. The treatment of asymptomatic hyperuricemia: results from the population based General Practice Research Database (GPRD). Arth Rheumtol 2003;48(Suppl. 9):S612.
12. Johnson RJ, Rideout BA. Uric acid and diet-insights into the epidemic of cardiovascular disease. N Engl J Med 2004;350:1071–3.
13. Underwood M. Clinical review: diagnosis and management of gout. BMJ 2006;332:1315–19.
14. Bomalaski JS, Clark MA. Serum uric acid-lowering therapies: where are we heading in management of hyperurecemia and the potential role of uricase. Curr Rheumatol Rep 2004;6:240–7.
15. Pacher P, Nivorozhkin A, Szabo C. Therapeutic effects of xanthine oxidase inhibitors: renaissance half a century after the discovery of allopurinol. Pharmocol Rev 2006;58:87–114.
16. Okamoto K, Eger BT, Nishino T, Kondo S, Pai EF. An extremely potent inhibitor of XOR, crystal structure of the enzyme inhibitor complex and mechanism of inhibition. J Biol Chem 2003;278:1848–55.
17. Kuang-Hui Yu. Febuxostate: a novel non-purine selective inhibitor of xanthine oxides for the treatment of hyperuricemia in gout. Recent Pat Inflamm Allergy Drug Discov 2007;1:69–75.
18. Nuki G, Simkin PA. A concise history of gout and hyperuricemia and their treatment. Arthritis Res Ther 2006;8:11–15.
19. Borges F, Fernandes E, Roleira R. Progress towards the discovery of xanthine oxidase inhibitors. Curr Med Chem 2002;9:195–217.
20. Terkeltaub RA. Clinical practice. Gout. N Engl J Med 2003;349:1647–55.
21. El-Assiery SA, Sayed GH, Fouda A. Synthesis of some new annulated pyrazolo-pyrido (or pyrano) pyrimidine, pyrazolopyridine and pyrano-pyrazole derivatives. Acta Pharm 2004;54:143–50.
22. Marel MG. Some reactions of pyrazolo(1,5-C)pyrimidinethiones. J Isla Acad Sci 1993;6(1):8–14.
23. Oliveira-Campos AMF, Salaheldin AM, Rodrigues LM. Synthesi of some novel pyrazolo(3,4-d)pyrimidine derivatives. ARKIVOC 2007;16:92–100.
24. Feigelson P, Davidson JD, Robins RK. Pyrazolopyrimidines as inhibitors and substrates of xanthine oxidase. J Biol Chem 1956;12:993–1000.
25. Rathish IG, Javed K, Ahmad S, Bano S, Alam MS, Pillai KK, et al. Synthesis and anti-inflammatory activity of some new 1,3,5-trisubstituted pyrazolines bearing benzene sulfonamide. Bioorg Med Chem Lett 2009;19:255–8.
26. Sidique S, Ardecky R, Ying Su, Narisawa S, Brown B, Millan JL, et al. Design and synthesis of pyrazole derivatives as potent and selective inhibitors of tissue-nonspecific alkaline phosphatase (TNAP). Bioorg Med Chem Lett 2009;19:222–225.
27. Shishoo CJ, Ravikumar T, Jain KS, Rathod IS, Gandhi TP, Satia MC. Synthesis of novel 1,2-(un)substituted-3-amino-5-aryl-6-arylaminopyrazolo[3,4-*d*] pyrimidine-4-(5*H*)-ones and their biological activity. Indian J Chem 1999;38(B):1075–85.
28. Kalwadia B, Ora S, Kishore W. Synthesis of condensed pyrido[1,2-a]-pyrimidine and pyrimido[4,5-d]pyrimidine derivatives from cyanoketene dithioacetal. Int J Chem Sci 2008;1:166–78.
29. Chen XB, Gomes MJ. Estimation of Microbial Protein Supply to Sheep and Cattle Based on Urinary Excretion of Purine Derivatives: An Overview of the Technical Details. Aberdeen, Scotland: International Feed Resources Unit, 1992:1–21.
30. Bergmeyer HU, Gawehn K, Grassl M. Enzymatic assay of Xanthine oxidase, In: Methods of Enzymatic Analysis, New York: Academic Press, 1974; 2 ed. I:521–2.
31. Tomohisa N, Hiroo Y, Takayuki F, Kazuki E, Haruhiko M. Novel xanthine oxidase inhibitor studies: Part 2. Synthesis and xanthine oxidase inhibitory activities of 2-substituted 6-alkyl-idenehydrazino- or 6-arylmethyllidenehydrazino-7*H*-purines and 3- and/or 5-substituted 9*H*-1,2,4-triazolo[3,4-i]purines. J Chem Soc Perkin Trans 1999;1: 3117–25.
32. BioMed Cache 6.1, Molecular Modeling Programme Package. Tokyo: Fujitsu Ltd, 2006.
33. Lipinski CA, Lombardo F, Dominy BW, Feeney PJ. Experimental and computational approaches to estimate solubility and permeability in drug discovery and development settings. Adv Drug Deliv Rev 2001; 46: 3–26.
34. Leal B, Afonso IF, Rodrigues CR, Abreu PA, Garrett R, Pinheiro LC, et al. Antibacterial profile against drug-resistance *Staphylococcus epidermidis* clinical strain and structure-activity relationship studies of 1*H*-pyrazolo[3,4-*b*]pyridine and thieno[2,3-*b*]pyridine derivatives. Bioorg Med Chem 2008;16:8196–204.
35. Sato T, Ashizawa N, Iwanaga T, Nakamura H, Matsumoto K, Inoue T, et al. Design, synthesis and pharmacological and pharmacokinetic evaluation of 3-phenyl-5-pyridyl-1,2,4-triazol derivatives as xanthine oxidoreductase inhibitors. Bioorg Med Chem Lett 2009;19:184–7.